

LETTER TO THE EDITOR

The rms-flux relation in accreting objects: not a simple ‘volume control’

A response to Koen 2016

Phil Uttley¹, Ian M. McHardy² and Simon Vaughan³

¹ Anton Pannekoek Institute, University of Amsterdam, Science Park 904, 1098 XH Amsterdam, The Netherlands
e-mail: p.uttley@uva.nl

² Physics and Astronomy, University of Southampton, Southampton SO17 1BJ, UK

³ Department of Physics and Astronomy, University of Leicester, Leicester LE1 7RH, UK

Received November 10, 2016

ABSTRACT

The light curves of a diverse range of accreting objects show characteristic linear relationships between the short-term rms amplitude of variability and the flux as measured on longer time-scales. This behaviour is thought to be imprinted on the light curves by accretion rate fluctuations on different time-scales, propagating and coupling together through the accretion flow. Recently, Koen (2016) proposed a simple mathematical interpretation for the rms-flux relation, where short-term variations are modulated by a single slower process. Here we show that this model was already considered and ruled out in Uttley et al. (2005), on the grounds that it did not produce the observed broad time-scale dependence of the rms-flux relation and associated lognormal flux distribution. We demonstrate the problems with the model via mathematical arguments and a case-study of Cyg X-1 data compared with numerical simulations. We also highlight another conclusion of our original work, which is that a linear rms-flux relation is easy to produce by a variety of models with positively skewed flux distributions. Observing such a relation in a non-accreting object (e.g. in solar flares) does not necessarily imply a phenomenological connection with the behaviour of accretion flows, unless the relation is seen over a similarly broad range of time-scales.

Key words. Accretion, accretion disks - Methods: statistical

1. Introduction

An apparently universal feature of the aperiodic ‘flickering’ flux variability seen from accreting compact objects is that they show a linear relationship between the rms amplitude of short-term variability and flux variations on longer time-scales. This so-called ‘rms-flux relation’ was first discovered by Uttley & McHardy (2001) in the X-ray light curves of X-ray binary systems (XRBs, both neutron star and black hole) as well as Active Galactic Nuclei (AGN). Since then, rms-flux relations have been found to be ubiquitous in the X-ray emission from black hole XRBs in different spectral states (Gleissner et al. 2004; Heil et al. 2012) and are also seen in the fast optical variability from hard state black hole XRBs (Gandhi 2009). Linear rms-flux relations are also present in the X-ray variability from ultraluminous X-ray sources (Heil & Vaughan 2010; Hernández-García et al. 2015) as well as the short time-scale optical variability of a blazar (Edelson et al. 2013). Expanding its scope beyond the most compact accreting objects, linear rms-flux relations are found in the broadband noise variability seen from accreting white dwarfs (Scaringi et al. 2012; Van de Sande et al. 2015; Dobrotka & Ness 2015) and even in young stellar objects (YSOs, Scaringi et al. 2015).

A very important and often not well-appreciated property of the rms-flux relation, is that in cases where data are good enough that it can be studied on different time-scales, it turns out that the linear rms-flux relation occurs *on all measured time-scales* (Ut-

ttley et al. 2005, henceforth UMV05). In other words, not only does the rms measured in short - e.g. 1 s - segments track the flux on longer time-scales (e.g. 10 s), but the rms variations produced on those longer time-scales also track the flux variations on even longer time-scales, e.g. minutes (see UMV05 and a more extensive discussion in Vaughan & Uttley 2008). This result has the corollary that the variability process is inherently non-linear and that, if the variability process is statistically stationary on long time-scales and stochastic fluctuations on different time-scales multiply together, the resulting (stationary) flux distribution should be lognormal. Such lognormal flux distributions are indeed observed from the data for X-ray binaries, AGN and accreting white dwarfs (Gaskell 2004, UMV05, Scaringi et al. 2012). All of these results tie in with the idea that the particular rms-flux relation seen in accreting systems is linked to the common feature: the accretion flow itself, with variations produced by turbulent fluctuations in mass accretion rate arising at different radii, which propagate through the flow so that variability is coupled together over and between a broad range of time-scales (Lyubarskii 1997; King et al. 2004; Arévalo & Uttley 2006; Ingram & van der Klis 2013; Scaringi 2014; Cowperthwaite & Reynolds 2014; Hogg & Reynolds 2016). It is possible that linear rms-flux relations are produced by other types of process but these are not expected to show the relation across and between a broad range of time-scales, as well as the corresponding lognormal flux distributions (see Appendix in UMV05 and Section 4 of this Letter).

Recently, Koen (2016) (henceforth K16) has proposed a simple model for the linear rms-flux relation seen from accreting objects. The K16 model invokes a simple scaling of a stationary statistical process so that the rms on the time-scales dominated by that process scales linearly with the scaling factor, which itself is time-variable. However, only two components couple together: the scaling factor is coupled to the short-term variability and there is no coupling of multiple variability components across a wider range of time-scales, as suggested by UMV05 and consistent with observations as well as predicted by models for accretion variability. It is therefore important to check whether this simple prescription is really a valid description of the observed light curves. Here we show that it is not and was in fact already discussed and ruled out by UMV05.

2. Koen’s model for the rms-flux relation

Following the notation of K16, the model can be written as:

$$X(t) = g(t)z(t), \quad (1)$$

where $g(t)$ is a ‘smooth trend’ while $z(t)$ is a more rapidly varying stationary stochastic process (K16 assume either a simple Gaussian independent and identically distributed variable, or a time-series produced by an autoregressive process). Thus, since the variations of $z(t)$ are assumed to be independent of those of $g(t)$, both the mean and the rms of variations of $X(t)$ on time-scales dominated by $z(t)$ will simply scale with the value of $g(t)$, to produce a linear rms-flux relation. However, while the K16 model limits the number of light curve components which must be multiplied together, this is also the downfall of the model, such that it does not reflect the observed light curve behaviour in accreting systems in two important ways.

Firstly, the K16 model does not predict that the rms-flux relation applies over and between a broad range of time-scales: the time-series $g(t)$ does not itself scale with another longer-time-scale time-series, contrary to what is seen in observed light curves of accreting objects. In fact, the model of K16 was already explicitly considered and rejected for this reason by UMV05 (see Section 3.2 of that paper), where it is described as being analogous to a simple ‘volume control’ on an amplifier or sound system. The rms amplitude of short-time-scale variations corresponds to the volume setting, which can itself be varied on longer time-scales. However, to reproduce the data, these longer time-scale variations would also need to follow a linear rms-flux relation (i.e. they must also be considered as a volume setting to be varied on even longer time-scales), with the amplitudes of those even longer time-scale variations modulated in the same way, and so on. This crucial ingredient is missing from the K16 model.

Secondly, the K16 model does not predict the observed lognormal flux distributions which (as shown in UMV05) arise from *stationary* time series when the rms-flux relation applies on all measured time-scales. This is simply because $\log[X(t)] = \log[g(t)] + \log[z(t)]$, so that $X(t)$ is only lognormally distributed if $g(t)$ and $z(t)$ are *both* also lognormally distributed, which would only be the case if they also followed linear rms-flux relations on all time-scales (UMV05). We note here that the simulated light curves presented in K16 are in any case not stationary and bear little resemblance to the ‘broadband noise’ or ‘flickering’ type light curves of real accreting sources (with similar amplitudes of variability per decade range in time-scale). It would be easy to adapt the K16 model so that the light curves are stationary, e.g. by using an autoregressive time-series model for $g(t)$. Such an

adaptation would still not produce the required lognormal flux distribution, however, unless both $g(t)$ and $z(t)$ are already lognormally distributed.

Finally, it is important to stress here that the fact that the rms-flux relation applies across a broad range of measured time-scales and that the flux distributions are lognormal are not merely ‘ingredients’ of the model of UMV05, they are observational results which support the interpretation that variations must multiply together over a broad range of time-scales. Any model which does not replicate those basic observational results (including the model of K16) is falsified, even if it can explain other aspects of the light curves such as the shape of the power spectrum.

3. A case study

To demonstrate that the K16 model for the rms-flux relation does not adequately describe the other key properties of the data described in the last section (lognormal flux distribution and linear rms-flux on a broad range of time-scales), *even while it can reproduce the observed power spectrum*, we now conduct a simple case-study using the Cyg X-1 December 1996 hard state Rossi X-ray Timing Explorer (*RXTE*) observations that were also used in UMV05. We will use this real light curve to determine the shape of the power spectrum and then generate a light curve using the K16 model to match the shape of the power spectrum. We will then demonstrate that the K16 simulated data shows a flux distribution and rms-flux relations which bear little resemblance to those of the real data. Finally we will demonstrate that the model of UMV05, where the flux is forced to be lognormally distributed, can reproduce the both the power spectrum and rms-flux properties of the real data.

For simplicity we obtained the ‘Standard 1’ light curves, which contain the net count-rate in 0.125 s intervals across all channels of the *RXTE* Proportional Counter Array (PCA). These light curves cover a broader energy range than the 2-13 keV band used in UMV05, but since the count rates are dominated by the softer energies, we do not expect this to make much difference to our results compared to UMV05 (and we confirm this to be the case). We chose the same relatively stationary section of the light curve used in UMV05, which includes a subset of the data from ObsIDs 10236-01-01-02, -020 and -021 with total exposure 38.5 ksec¹.

As we have already noted, the K16 model assumes a deterministic long time-scale driving time-series $g(t)$. Such a time-series model, with large long-term variability trends and a correspondingly steep power spectrum, does not produce power spectra resembling those of real accreting sources, which in the hard state of black hole XRBs resemble a sum of broad Lorentzian components (Pottschmidt et al. 2003). Therefore for the K16 model we instead assume a more plausible driving signal, where the lowest-frequency Lorentzian in the broadband PSD is assumed to drive the variations of the sum of the higher-frequency Lorentzians. To construct the model we first fit the power-spectrum of the real data, with three broad Lorentzian components, using the model prescription of Pottschmidt et al. (2003). We allow all parameters (Lorentzian peak frequency, integrated fractional rms and the frequency coherence q) to vary except q for the highest-frequency Lorentzian, which we fix to $q = 0.3$ since this component lies at the edge of the measured frequency range and is otherwise degenerate in its parameters.

¹ This is ~20 per cent longer than the light curve used in UMV05, due to more stringent good-time-intervals used in that paper, which are relaxed now that the *RXTE* mission calibration has matured.

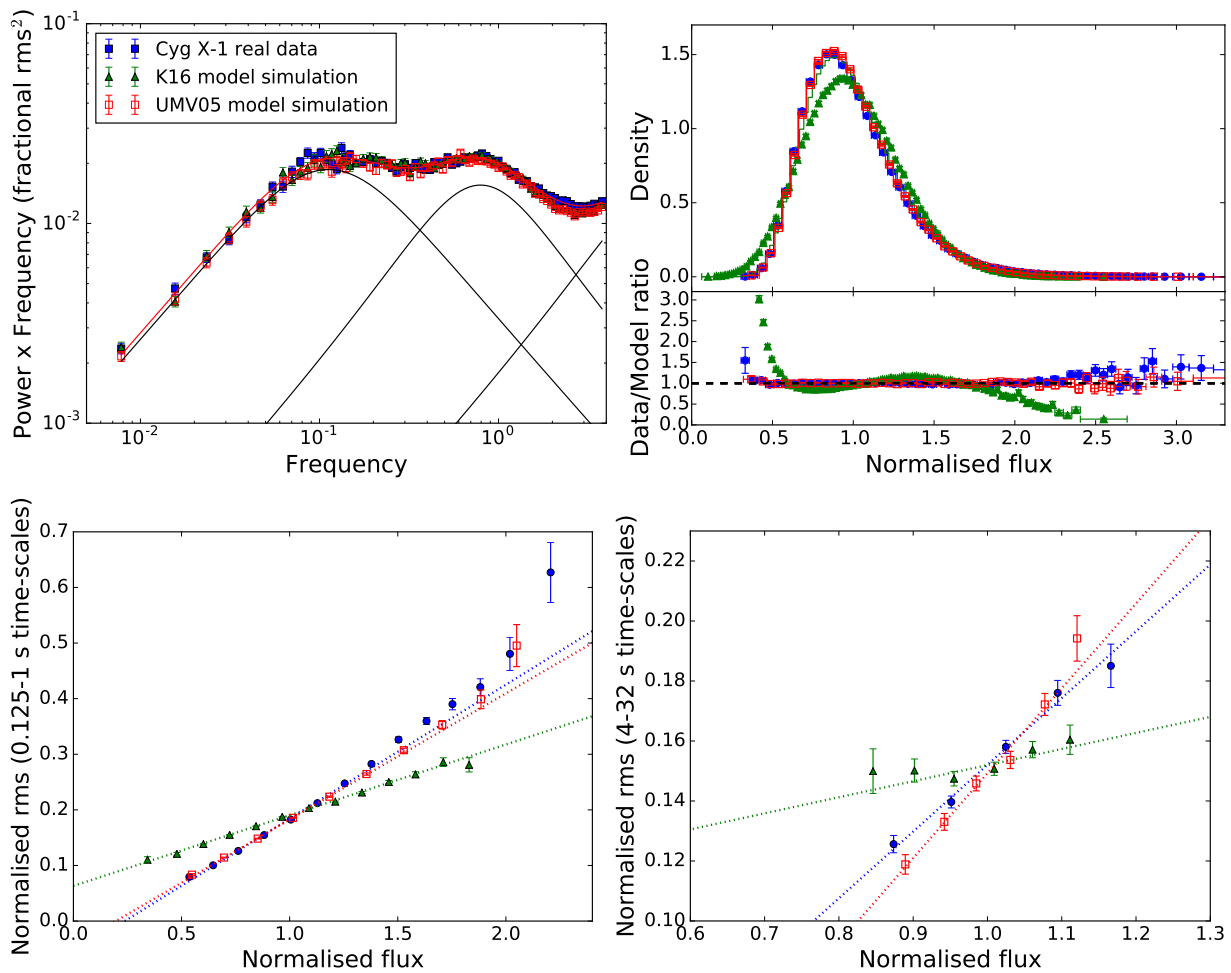


Fig. 1. Comparison of real Cyg X-1 hard state data (blue circles) with simulated data showing the same power spectrum, made using the K16 model (green triangles) or the ‘exponentiated’ model of UMV05 (open red squares). *Top left:* power spectra of the light curves, including the best-fitting Lorentzian decomposition for the real data (black lines, total model line in solid red). *Top right:* flux distributions (flux normalised by mean count rate), models (coloured lines) and data/model ratios for a fit to a lognormal model with constant offset constrained to be non-negative. *Bottom panels:* the rms-flux relations of the light curves obtained for rms measured on two different time-scale ranges, short (0.125-1 s, *bottom left panel*) and long (4-32 s, *bottom right panel*). Best-fitting linear (plus constant) relations are also shown as dotted lines. For the flux distributions and rms-flux relations, the K16 model is strongly inconsistent with the data, while the UMV05 model works reasonably well.

The resulting fit is reasonable given the simplicity of the model and good data quality ($\chi^2 = 81.3$ for 67 d.o.f.) and the data and best-fitting model (including the decomposition in terms of separate Lorentzians) is shown in Fig. 1 (top left panel).

We next confirmed one of the key results of UMV05 by fitting a three-parameter lognormal model to the flux distribution of the real light curve (flux is normalised by the mean count rate). The observed distribution, best-fitting model (see UMV05 for the model description) and data/model ratio are shown in Fig. 1 (top right panel). The lognormal model provides a good fit to the data over most of the measured flux range, although the fit is poorer in the tails of the distribution (resulting in $\chi^2 = 86.6$ for 52 d.o.f., similar to the quality obtained by UMV05)². These deviations may result from a number of subtle aspects of the data, e.g. the fact that the light curve is not strictly stationary or perhaps real physical effects not accounted for by such a simple

² Best-fitting parameters are shape parameter $\sigma = 0.36$, location parameter $\tau = 0.16$ and scale parameter $\ln(\mu) = 0.79$. We do not quote errors on these values since the fit is not formally acceptable, but we note that they are consistent with the parameters obtained by us for the fit in UMV05

mathematical model. Nevertheless, we will see that the lognormal fit is a much better match to the data than to a simulated light curve based on the K16 model.

To simulate the K16 version of the light curve, we used the approach of Timmer & Koenig (1995) to simulate zero-mean Gaussian flux distributed light curves (with the same length as the original data) for each of the three Lorentzian components (using the Lorentzian parameters obtained from the fit to the real data), which we call (in order of frequency) $l_1(t)$, $l_2(t)$ and $l_3(t)$. We then construct the K16 model light curve as follows:

$$X_{K16}(t) = (1 + l_1(t))(1 + l_2(t) + l_3(t)) \quad (2)$$

i.e. $l_1(t)$ subsumes the role of the slowly varying time-series $g(t)$ (although in this case, it is Gaussian distributed and stationary - the latter being required to fit the power spectrum), while $(l_2(t) + l_3(t))$ takes the role of the short-term Gaussian-distributed component $z(t)$. Finally, we scaled the light curve to the observed mean count rate and included Poisson noise. The power spectrum of this K16 simulated light curve is also included in Fig. 1 (top left panel), which shows that it is a close match to the power spectrum of the real data.

We next fitted the lognormal model to the flux distribution of the K16 light curve. If we apply no constraints to the model parameters, we can return a reasonable fit, but only with negative values of the location parameter, which when combined with a large scale-parameter can produce distributions which are close to normally distributed, rather than pure lognormal. However this situation would correspond to unphysical negative constant offsets in the flux distribution, as opposed to the physically plausible situation of a positive offset as seen in the real data, which could be explained by the presence of a constant-flux component. Therefore we restrict the offset τ to be > 0 , which makes the fit to the lognormal model much worse than seen in the real data (as can be seen Fig. 1, top right panel).

We also compared the rms-flux relations of the light curves obtained for two different time-scales. The short-term rms-flux relation was obtained by binning the variance obtained in 1 s segments according to flux (then subtracting the expected Poisson noise contribution and taking the square-root to get the rms). The long-term rms-flux relation was obtained by first binning up the 0.125 s resolution light curves to 4 s resolution, and then measuring the rms-flux relation in the same way as for the short-term relation, except using 32 s segments. Thus the short-term relation is driven by the sub-second rms of the l_2 and l_3 Lorentzians responding to modulation by the l_1 Lorentzian, while the long-term rms is dominated more by the l_1 Lorentzian which is not modulated by any additional time-scales.

The rms-flux relations are shown in the bottom panels of Fig. 1. As expected, both the real data and the K16 model light curves show close to linear short-term rms-flux relations, although the slope for the K16 simulation is significantly flatter than in the real data, which is likely due to the contribution of the l_1 Lorentzian to the sub-second variability (since it adds an rms component which does not depend on the flux). The long-term rms-flux relation of the K16 model light curve is close to being constant, rather than linear, which is as expected since this component does not have any rms-flux relation built in due to variations on even longer time-scales. In contrast, the real data show a clear linear rms-flux relation on both long and short time-scales.

For comparison, we also simulated a light curve using the ‘exponentiation’ approach of UMV05, which is designed explicitly to produce the observed lognormal flux distribution seen in the data and hence (as shown in UMV05) also produce the linear rms-flux relations seen on all time-scales. The model works simply by taking the exponential of a Gaussian-distributed time-series such that the resulting flux distribution is lognormal. In the case of our multiple-Lorentzian power spectrum, the operation is simply to take the exponential of the sum of (zero-mean) simulated Lorentzian light curves generated using the Timmer & Koenig (1995) approach, i.e.:

$$X_{\text{exp}}(t) = \exp(l'_1(t) + l'_2(t) + l'_3(t)) \quad (3)$$

The primes denote that we followed the approach of UMV05 in reducing the amplitudes of the input Lorentzians used to make the original Gaussian-distributed light curves, to account for the effect of exponentiating the combined light curve (since this transformation increases the rms amplitude). Besides ensuring that the final fractional rms matches that of the data, we also choose the lognormal location parameter $\tau = 0.16$, to match that of the real data. We apply the same analysis as for the real data and K16 simulation and the results are included in all the plots in Fig. 1.

The exponentiated light curve shows a similar power spectrum to the real data and has a lognormal flux distribution by

construction which, as expected, looks very similar to that of the real data. The rms-flux relations are also similar to those of the real data on both long and short time-scales. There are small differences but these are expected given that the exponentiation approach is very simplified, while real data shows more complex behaviour (e.g. in higher-order statistics such as the bicoherence, UMV05). In conclusion, our simulated exponentiated light curve shows a flux distribution and rms-flux relations which appear more similar to the real data than the K16 model light curve does. Thus, our simulations demonstrate the arguments made in the previous section.

4. Some final remarks

It is important to note that a linear rms-flux relation, by itself, is not evidence for the same kind of variability process which produces lognormal flux distributions and linear rms-flux relations across a broad range of time-scales. As noted in UMV05 (see Appendix D of that paper), linear rms-flux relations can result generally from light curves with positively skewed flux distributions, provided that the rms which is plotted versus flux corresponds to a large fraction of the total variability amplitude (i.e. the rms of segments is relatively large compared to the amplitude of variations which produce the variations in mean flux of the segments). This situation can occur in time-series which do not have very broad power spectra, unlike those seen in accreting objects where a broad range of frequencies contribute similar amounts to the total variability amplitude. This property of time series with positively skewed flux distributions and relatively narrow-band power spectra can explain the presence of linear rms-flux relations in models distinct from the propagating fluctuations model, such as the ‘thundercloud model’ of Merloni & Fabian (2001). This effect can also explain the presence of linear rms-flux relations in diverse data such as light curves of solar flares (Zhang 2007), where the rms variability amplitude in 1 s intervals is of a similar order to the highly skewed and non-linear flux variation on longer time-scales. The presence of linear rms-flux relations should therefore not be taken as an indication of similar variability processes to those seen in accreting systems, unless the effects of the flux distribution and power-spectral shape are also accounted for.

References

- Arévalo, P. & Uttley, P. 2006, MNRAS, 367, 801
 Cowperthwaite, P. S. & Reynolds, C. S. 2014, ApJ, 791, 126
 Dobrotka, A. & Ness, J.-U. 2015, MNRAS, 451, 2851
 Edelson, R., Mushotzky, R., Vaughan, S., et al. 2013, ApJ, 766, 16
 Gandhi, P. 2009, ApJ, 697, L167
 Gaskell, C. M. 2004, ApJ, 612, L21
 Gleissner, T., Wilms, J., Pottschmidt, K., et al. 2004, A&A, 414, 1091
 Heil, L. M. & Vaughan, S. 2010, MNRAS, 405, L86
 Heil, L. M., Vaughan, S., & Uttley, P. 2012, MNRAS, 422, 2620
 Hernández-García, L., Vaughan, S., Roberts, T. P., & Middleton, M. 2015, MNRAS, 453, 2877
 Hogg, J. D. & Reynolds, C. S. 2016, ApJ, 826, 40
 Ingram, A. & van der Klis, M. 2013, MNRAS, 434, 1476
 King, A. R., Pringle, J. E., West, R. G., & Livio, M. 2004, MNRAS, 348, 111
 Koen, C. 2016, A&A, 593, L17
 Lyubarskii, Y. E. 1997, MNRAS, 292, 679
 Merloni, A. & Fabian, A. C. 2001, MNRAS, 328, 958
 Pottschmidt, K., Wilms, J., Nowak, M. A., et al. 2003, A&A, 407, 1039
 Scaringi, S. 2014, MNRAS, 438, 1233
 Scaringi, S., Kording, E., Uttley, P., et al. 2012, MNRAS, 421, 2854
 Scaringi, S., Maccarone, T. J., Kording, E., et al. 2015, Science Advances, 1, e1500686
 Timmer, J. & Koenig, M. 1995, A&A, 300, 707
 Uttley, P. & McHardy, I. M. 2001, MNRAS, 323, L26
 Uttley, P., McHardy, I. M., & Vaughan, S. 2005, MNRAS, 359, 345
 Van de Sande, M., Scaringi, S., & Knigge, C. 2015, MNRAS, 448, 2430
 Vaughan, S. & Uttley, P. 2008, ArXiv e-prints [arXiv:0802.0391]
 Zhang, S. N. 2007, Highlights of Astronomy, 14, 41